SCEC Report: Proposal 20068

Rock towers as ground motion constraints: A case study of the Trona Pinnacles fragile geologic features in the wake of the 2019 Ridgecrest sequence

PIs: Domniki Asimaki (Caltech), Devin McPhilipps (USGS Pasadena)
Postdoctoral Researcher: Joaquin Garcia Suarez (Caltech)

Abstract

Fragile geologic features, such as precariously balanced rocks (PBRs), have been used to constrain the intensity of past earthquake shaking. We analyzed the seismic response of another category of fragile geologic features, rock towers (RTs), using high-resolution, finite-element simulations. RTs differ from PBRs because RTs are materially connected to bedrock at their bases. We conducted the simulations using cm-resolution photogrammetric shape models and compared the results to paired broad-band seismic recordings from RTs and far-field bedrock as well as other field observations at the Trona Pinnacles, a group of RTs in southern California. The results of our simulations capture the first vibrational mode and the magnitude of amplification. However, simulations predict an important second vibrational mode, which was not observed. We interpret the differences to result from variations in material properties such as density and stiffness. Simulations also indicate that peak stresses occur near the base of the RT during earthquake shaking. Ongoing work aims to constrain the probability of intensity measure exceedance through dynamic modeling of a RT toppling, given shaking intensity, geometric parameters, and bulk tensile strength.

Introduction

Probabalistic Seismic Hazard Analysis (PSHA) quantifies the probability of exceedance of a ground motion intensity measure at a site within a time horizon. Fragile geological features (FGFs) allow us to pose a contradiction test over seismic hazard models and their predicted ground motions: dating experiments of these features can be used to contradict PSH models that predict high probability of events which, should they have taken place, unequivocally would have led to the failure of these features. While precariously-balanced rocks have been used in the recent past to constraint PSHAs (Rood et al., 2020, among others), the seismic capacity and evolution of rock towers (RTs) studied here has received much less attention. This report addresses the necessity of a better understanding of tower's response and evolution using numerical and analytical tools, which we use to analyse instrumented

such features and to put forward hypotheses to be tested in future work. Even though the study of these rock formations has been framed as a means to an end (better hazard assessment) thus far, their study possess interest in and of itself. This work can also shed light, for instance, over reasons behind the particular geometries that are observed in the field, and on how the shapes of the pinnacles evolve over time.

Previous work

The most widely used simplified models of fragility estimation of FGFs are based on quasi-static analyses of Euler-Bernoulli beams. Similarly, seismic stability of speleothem formations or hooboos(Anooshehpoor et al., 2013; Mendecki and Szczygieł, 2019) is analyzed in the same vein: resisting forces due to the strength and mass of the pillar are assumed to balance the inertia load. In a recent such study by McPhillips and Scharer (2019) for example, fragility data were collected for 47 rock pillars in southern Oregon, where ground motion constraints are particularly valuable for physics-based simulations of megathrust events in the Pacific Northwest subduction zone. McPhillips and Scharer (2019) define a rock pillar as any natural feature with a high aspect ratio and a material connection to bedrock at one end. Forty of the pillars in their study are sea stacks located along the coast from Bandon to Brookings. The remainder seven consist of various pillars located farther inland, including volcanic plugs and speleothems. The data they collected describe size, shape, orientation, lithology, and tensile strength of these features. Next, they used this database to estimate the minimum quasi-static horizontal acceleration required to break the pillars at the base. The critical parameters were identified as the height of the center of mass, the second moment of area, the mass, and the tensile strength. The first two parameters are a function of shape, which was modeled as either a rectangular prism or elliptical frustum and measured using a tape, laser rangefinder, and clinometer. For two pillars, volumes were also calculated from structure from motion (SfM) photogrammetry, and the results agreed with the simple models to within 15%. Mass was estimated from shape and density, which in turn was estimated from lithological observations; tensile strength was estimated using more than 1000 rebound hammer measurements. There is an extensive literature for measuring unconfined compressive strength with rebound hammers in natural rock samples (Wang et al., 2017), and this value may be scaled to tensile strength (Perras and Diederichs, 2014), provided that appropriate scaling is applied to account for the sample size (Anooshehpoor et al., 2013).

The Trona Pinnacles FGFs, which experienced damage during the 2019 Ridgecrest earthquake sequence, offer a unique opportunity to evaluate simplified methods of extracting realistic fragility data from databases of FGFs; to validate high fidelity finite element models of these pinnacles by comparing simulated to measured dynamic characteristics; and to evaluate the reliability of quasi-static simplified fragility models by comparing with dynamic, elastoplastic FEM simulations of the pinnacle response to earthquake shaking.

A summary of our work in progress is outlined in the ensuing of this report, focusing on one of the instrumented pinnacles that we hereafter will refer to as *skinny*.

Progress report

The Trona pinnacle system is located approximately 10 miles southeast of Ridgecrest, CA. There are over 500 of these formations over an area of 14 square miles, scattered over the ancient Searles Lake basin, and ranging from small boulders to over 40-meter tall slender features. In terms of geometry, they present different degrees of slenderness, and, for the most part, their overall shape is either cylindrical or resembling an inverted cone. This unusual landscape was declared National Natural Landmark by the U.S. Department of the Interior in 1968 [1].

Instrumentation and material properties

To capture the field vibration characteristics of *skinny*, the feature was instrumented with Trillium seismometers from the USGS Pasadena Office in the wake of the Ridgecrest aftershock sequence. These measurements will be used in the following sections to evaluate our numerical model capability to capture vibration characteristics and dynamic response to seismic loading.

Trona pinnacles are composed of calcium carbonate (tufa); slender pinnacles such as *skinny* can be considered homogeneous for modeling purposes, an assumption that we confirmed when comparing simulations to field measurements of pinnacle vibrations. Schmidt hammer testing (Wang et al., 2017) was employed to characterize the material unconfined compressive strength by reducing the measurements by 50% to take into account size effects (larger fractures than in the sample (Anooshehpoor et al., 2013). The unconfined compressive strength can then be related to direct tensile strength (Perras and Diederichs, 2014), while there are similar scaling laws available regarding the elastic modulus (Aydin and Basu, 2005). Recent work by Sopaci and collaborators was used as a reference (Sopacı and Akgün, 2015; Sopacı et al., 2019) to compare with and complement our field property measurements. For a number of possible types of tufa in the region under study, Sopacı et al. (2019) reported average Young's modulus in the range $E \sim 0.6\,\text{GPa}$ to $\sim 13.3\,\text{GPa}$, and average Poisson's ratio in the range $\nu = 0.03$ to 0.29. In terms of tensile strength, the Sopacı et al. (2019) laboratory mean Brazilian tensile strength ranges from 1.2 MPa to 3.1 MPa (depending on the type of tufa), while field tests yielded 0.9 MPa. Note that this finding is analogous to the scale effects observed by (Anooshehpoor et al., 2013) for the unconfined compression strength (Yoshinaka et al., 2008).

As a first level of abstraction, one can idealize the pinnacle using Timoshenko beam theory, which decouples the bending phenomenon from the shearing of the cross-sections.

[1] Bureau of Reclamation, available at `https://www.blm.gov/visit/trona-pinnacles`, Last visited on 14/9/2020

Considering that the wavelength of the excitation is much larger than the pinnacle dimensions, its response to this load is expected to be global: the pinnacle likely deformed as a coherent whole during the Ridgecrest ground shaking, accommodating bending deformation easily by successive rotations of the cross-sections with little relative shearing. We confirm this dominant modal shape in the following sections.

Finite element model (FEM)

Point cloud from photogrammetry measurements was used to generate a finite element mesh (FEM) of *skinny* in Mathematica. We first used the FEM to analyze the natural frequencies of the feature and interpret the deformation field (vibration mode) and the period of oscillation (natural frequency) at which the feature is expected to vibrate when excited dynamically at the base. The expectation here is that if resonance is triggered, the response will significantly depart from the quasi-static conditions that form the basis of empirical FGF fragility models.

For this analysis, we assumed linear elastic material properties in accordance with the discussion in the previous section, namely: $\rho = 1700\,\mathrm{kg/m^3}$ (density), $\nu = 0.15$ (Poisson's ration), $E = 1.7\,\mathrm{GPa}$ (Young's modulus); and used the *Mathematica* function `NDEigensystem` with default settings (aka. the Arnoldi method) to extract the natural vibration information, unless otherwise stated explicitly. Figure 1 depicts the modal shapes of the first three modes; the two first vibration shapes correspond to bending modes (as expected based on the pinnacle aspect ratio), while the third one is a torsional mode. The resonant frequency of this torsional mode is so high that it is unlikely that a seismic load may excite it enough to trigger failure.

Including the compliant base of the pinnacle is expected to significantly reduce these frequencies. For this pinnacle, we include a cuboid of 6x6 square-meter cross-section (centered at the pinnacle's center of mass) with a 4-meter depth. The material is assumed to be the same as the pinnacle. Table 1 shows that the fixed base model has natural frequencies 25% higher than the model with complying base. The third one (torsional mode) is not as strongly affected by the compliant base, suggestive of the fact that the surrounding soil does not provide as much additional compliance for this type of deformation. This phenomenon of frequency shift when the compliant base is included is referred to in the field of soil-structure interaction as 'period lengthening'. We should also note that while the modal frequencies are significantly affected, the modal shapes are the same (compare Figure 1 to Figure 2).

Table 1: Influence of surroundings over Skinny's vibration modes.

	Linear Model (units: Hz)		
	First Mode	Second Mode	Third Mode
W/o pedestal	16.61	18.07	50.5
W/ pedestal	12.99	14.07	45.2
Difference (%)	27.8	28.4	11.7

Model validation: Dynamic analyses

We first validate the predicted resonant properties of the model. Figure 3 presents response spectral ratio of pinnacle deformation relative to an adjacent rock outcrop reference station. A clear amplification in the interval 12 to 14 Hz is revealed, consistent with the frequencies of the first two modes of the pinnacle/pedestal ensemble predicted by FEM, namely 13 Hz and 14 Hz. This result serves as a preliminary verification of the numerical model.

We next validate our numerical model by comparing the predicted response to the recorded transient response of the pinnacle during an Mw 1.9 aftershock of the Ridgecrest sequence. The 3-component reference station input motion is introduced to the pinnacle model as a prescribed plane stress wave through the domain reduction method. Far-field boundary reflections are minimized by the use of lysmer absorbing boundaries conditions. All these features are available in the open source Finite Element Analysis code Seismo-VLAB (`www.seismovlab.com`).

Figure 4 compares the velocity time history at the top of the tower overlying the recorded pinnacle response at the same location. The main features to note are:

1. The high-frequency oscillations are not fully captured, while the general trend in the records is resembled by the simulations.

2. The local maxima in the original records (at approximately 2s in the simulation) is understimated by the numerics.

3. Beating phenomenon appears in the FEM response due to the existence of two dominant modes with very similar frequencies. The real response does not present this phenomenon, at least not so markedly, as the two bending modes are more distanced from each other than in the numerical model.

Computing the FFT of both time responses yields the results in Figure 5, which reinforce the points above. There are two main peaks, with different degree of separation between them depending on being either the simulation or the actual record.

The fact that the third mode (torsion, around 40 Hz) does have a distinguishable contribution (in particular along the north direction) hints the possibility of the numerical model lacking a damping mechanism: the only energy-dissipation mechanism included in the current model is radiational damping, no internal damping is included at the material

level. For instance, the hysteretic damping that is customarily used in soil mechanics bundles a number of different of dissipative phenomenon (plasticity, fracture, heating...) that may occur simultaneously at the lower material scales. Such features are not included in the numerical analysis, and they have to be relevant, in light of these results.

The main conclusion to be attained from this suite of numerical simulations is that the finite-element model is able of capturing the main traits of the real response as observed in field data, so let these results served as validation of our model. This positive statement comes with a caveat: even though the current numerical tools can predict the general features, they cannot do so for the exact time-history for a given event.

The latter issue does not arise solely from limitations of numerical modeling: there is a component of uncertainty coming from the modeling of the input, as our choice of decoupled plane waves impinging normally on the free surface is not the only possibility (yet the simplest one) when it comes to reenact the ground shaking measured by the free-field seismometer.

REFERENCES

Anooshehpoor, A., Brune, J. N., Daemen, J., and Purvance, M. D. (2013). Constraints on ground accelerations inferred from unfractured hoodoos near the garlock fault, california. *Bulletin of the Seismological Society of America*, 103(1):99–106.

Aydin, A. and Basu, A. (2005). The schmidt hammer in rock material characterization. *Engineering Geology*, 81(1):1–14.

McPhillips, D. and Scharer, K. (2019). Preliminary survey of fragile geological features for use as ground motion constraints, southern oregon. *Southern California Earthquake Center Annual Meeting, Poster 290, Palm Springs, California.*

Mendecki, M. and Szczygieł, J. (2019). Physical constraints on speleothem deformations caused by earthquakes, seen from a new perspective: Implications for paleoseismology. *Journal of Structural Geology*, 126:146–155.

Perras, M. A. and Diederichs, M. S. (2014). A review of the tensile strength of rock: concepts and testing. *Geotechnical and geological engineering*, 32(2):525–546.

Rood, A., Rood, D., Stirling, M., Madugo, C., Abrahamson, N., Wilcken, K., Gonzalez, T., Kottke, A., Whittaker, A., Page, W., et al. (2020). Earthquake hazard uncertainties improved using precariously balanced rocks. *AGU Advances*, 1(4):e2020AV000182.

Sopacı, E. and Akgün, H. (2015). Geotechnical assessment and engineering classification of the antalya tufa rock, southern turkey. *Engineering Geology*, 197:211–224.

Sopacı, E., Akgün, H., and Daemen, J. J. (2019). An empirical strength criterion for the antalya tufa rock, southern turkey. *Environmental Earth Sciences*, 78(18):567.

Wang, H., Lin, H., and Cao, P. (2017). Correlation of ucs rating with schmidt hammer surface hardness for rock mass classification. *Rock Mechanics and Rock Engineering*, 50(1):195–203.

Yoshinaka, R., Osada, M., Park, H., Sasaki, T., and Sasaki, K. (2008). Practical determination of mechanical design parameters of intact rock considering scale effect. *Engineering Geology*, 96(3-4):173–186.

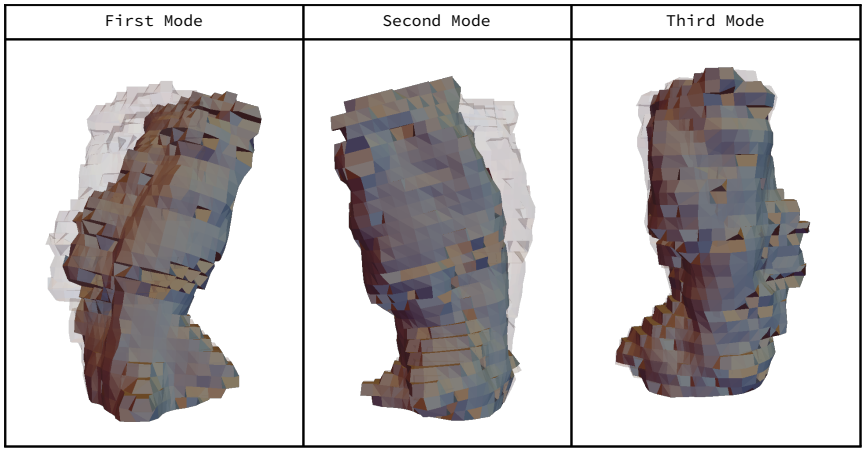

Figure 1: First, second and third vibration shapes of the isolated pinnacle.

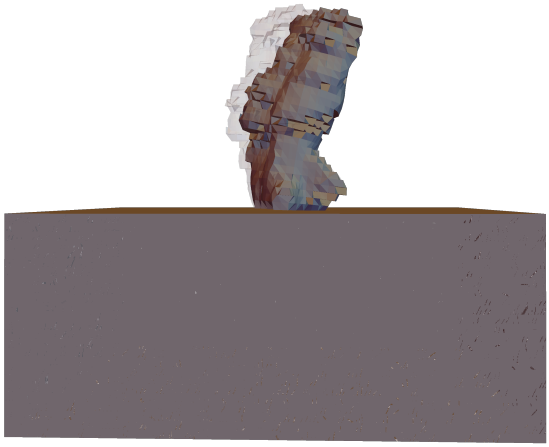

Figure 2: Fundamental mode shape of Skinny when including surroundings.

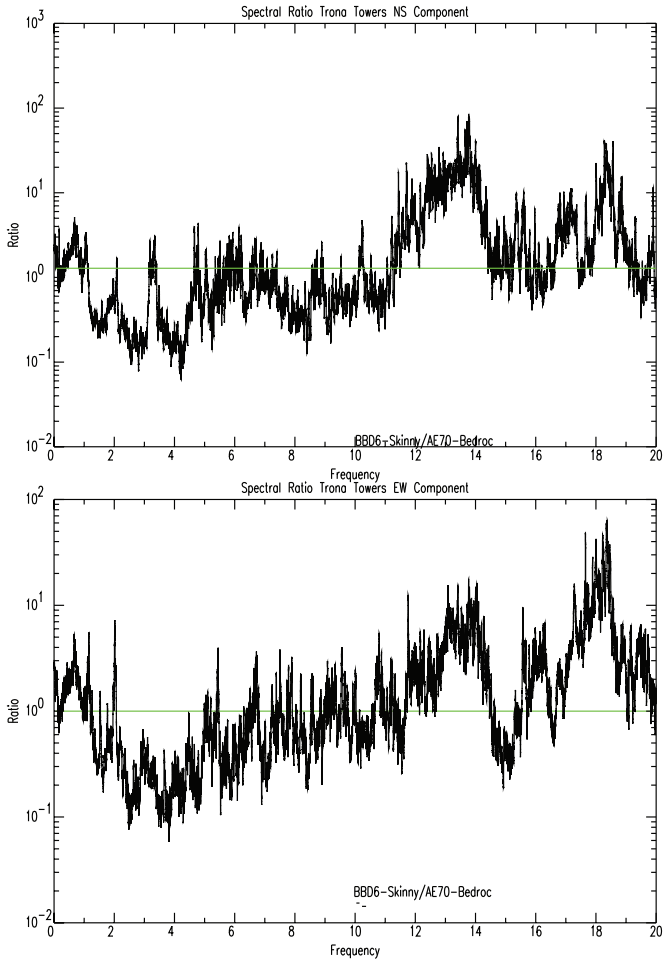

Figure 3: Spectral ratios for North-South and East-West components of Skinny's ambient vibration.

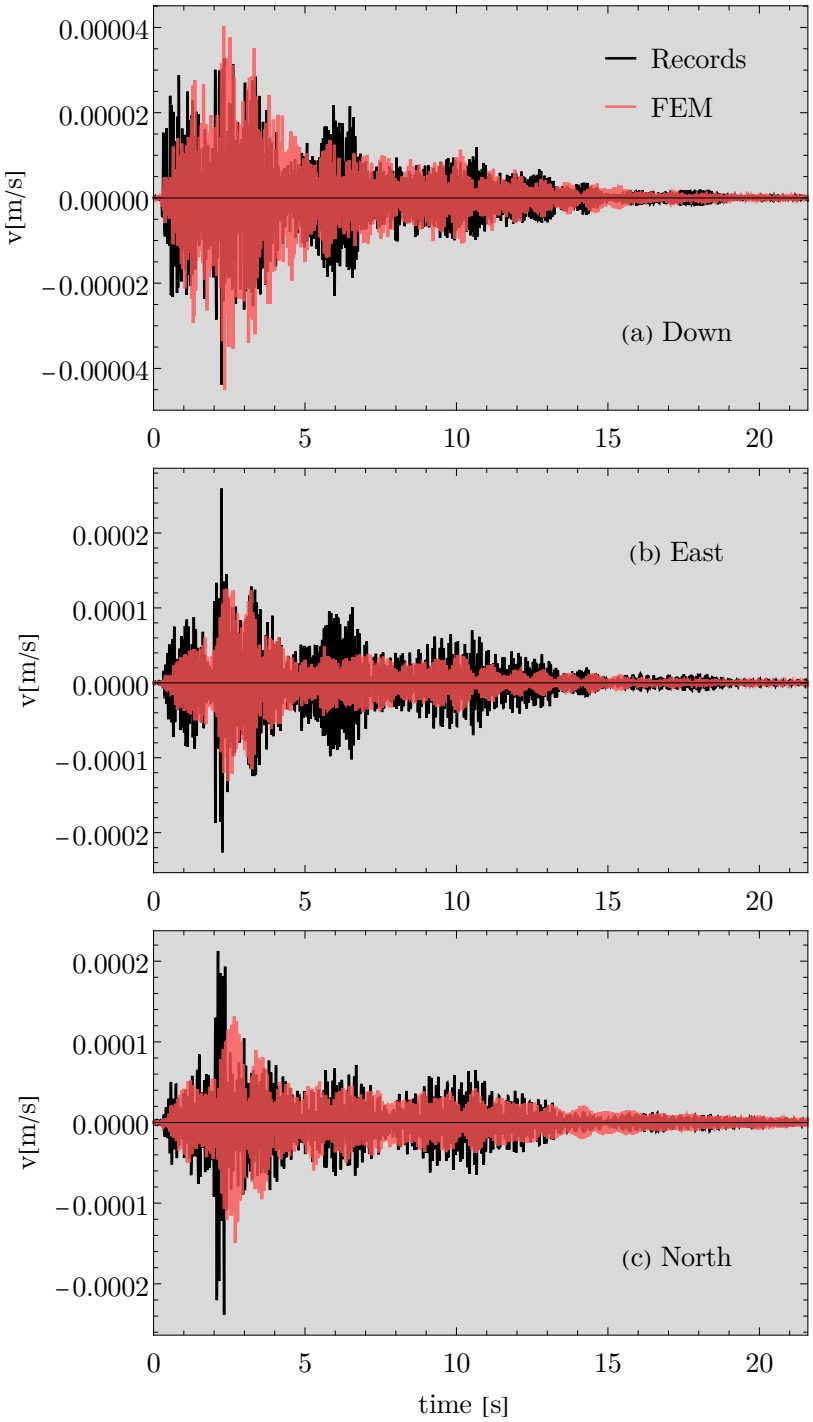

Figure 4: Numerical response v. recorded response (Skinny).

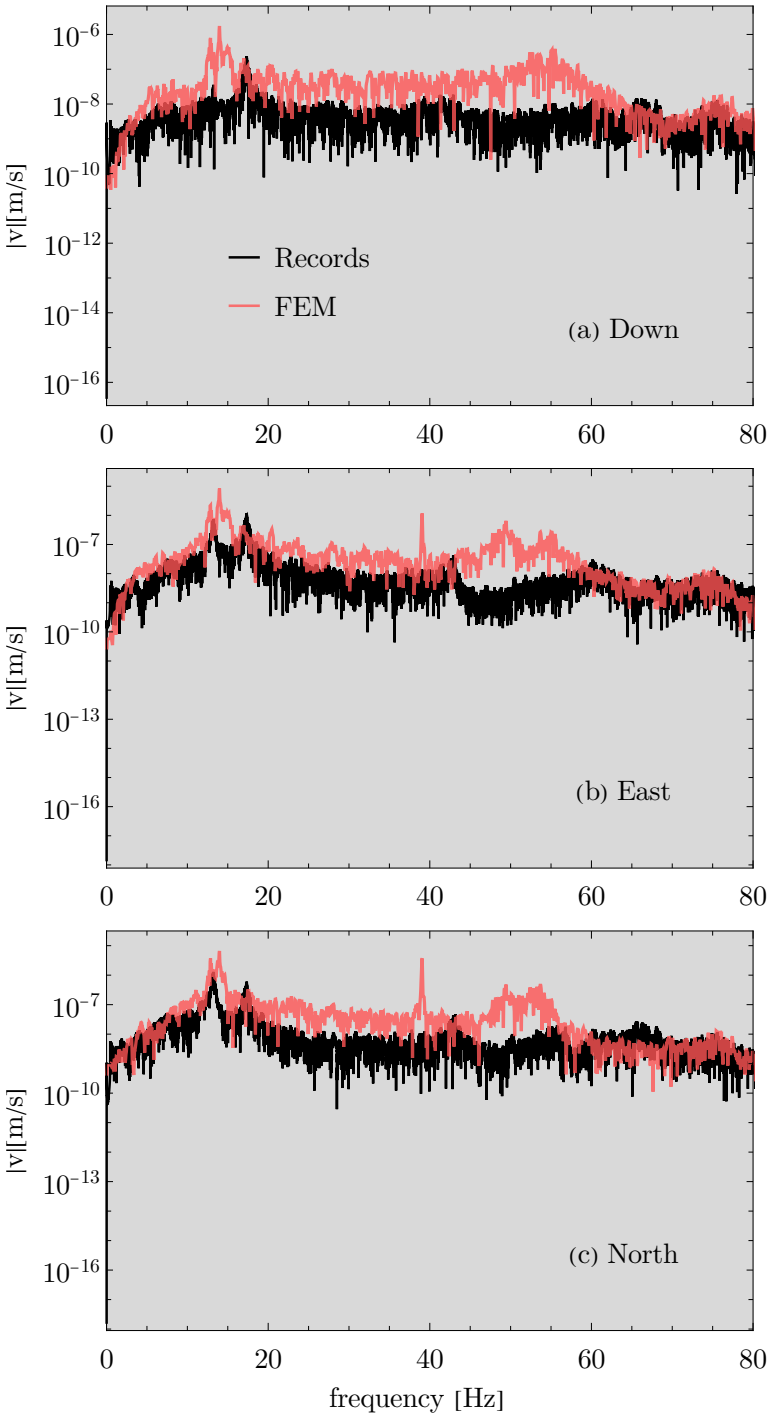

Figure 5: One-sided spectrum of the records in fig. 4.